CERN-PH-TH/2008-197
UAB-FT-654
FERMILAB-PUB-08-317-T
ANL-HEP-PR-08-33
EFI-08-16

The Baryogenesis Window in the MSSM

M. Carena [a,f,h], G. Nardini [b], M. Quirós [b,c,d], C.E.M. Wagner [e,f,g,h]

[a] *Fermi National Accelerator Laboratory, Batavia, IL 60510, USA*
[b] *IFAE, Universitat Autònoma de Barcelona, 08193 Bellaterra, Barcelona, Spain*
[c] *Instituciò Catalana de Recerca i Estudis Avancats (ICREA)*
[d] *Theory Division, Physics Department, CERN CH-1211 Geneva 23, Switzerland*
[e] *HEP Division, Argonne National Laboratory,Argonne, IL 60439, USA*
[f] *Enrico Fermi Institute and* [g] *Kavli Institute for Cosmological Physics*
[h] *Physics Department, University of Chicago, Chicago, IL 60637, USA*

Abstract

Electroweak baryogenesis provides an attractive explanation of the origin of the matter-antimatter asymmetry that relies on physics at the weak scale and thus it is testable at present and near future high-energy physics experiments. Although this scenario may not be realized within the Standard Model, it can be accommodated within the MSSM provided there are new CP-violating phases and the lightest stop mass is smaller than the top-quark mass. In this work we provide an evaluation of the values of the stop ($m_{\tilde{t}}$) and Higgs (m_H) masses consistent with the requirements of electroweak baryogenesis based on an analysis that makes use of the renormalization group improved Higgs and stop potentials, and including the dominant two-loop effects at high temperature. We find an allowed window in the $(m_{\tilde{t}}, m_H)$-plane, consistent with all present experimental data, where there is a strongly first-order electroweak phase transition and where the electroweak vacuum is metastable but sufficiently long-lived. In particular we obtain absolute upper bounds on the Higgs and stop masses, $m_H \lesssim 127$ GeV and $m_{\tilde{t}} \lesssim 120$ GeV, implying that this scenario will be probed at the LHC.

1 Introduction

The minimal supersymmetric extension of the Standard Model (MSSM) has become the preferred candidate for the Standard Model (SM) ultraviolet completion beyond the TeV scale. The MSSM provides a well defined and consistent perturbative framework which may be extended up to a high (GUT or Planck) energy scale. Among its main virtues, on top of solving the SM hierarchy problem, the MSSM is consistent with precision electroweak data, it leads to a natural unification of the three gauge couplings, and provides a natural candidate for the Dark Matter of the Universe, namely the lightest neutralino. The search for supersymmetric particles is therefore one of the main experimental goals at the forthcoming Large Hadron Collider (LHC) at CERN.

On the other hand electroweak baryogenesis [1]-[5] is a very elegant mechanism for generating the Baryon Asymmetry of the Universe (BAU) that relies on physics at the weak scale and can therefore be tested at present accelerator energies, in particular at the Tevatron and the LHC. It has been shown that electroweak baryogenesis cannot be realized within the Standard Model framework [6]-[10], and it is neither feasible in the MSSM for arbitrary values of its parameters [11]-[13]. A particular region in the space of supersymmetric mass parameters was found in the MSSM, where electroweak baryogenesis has the potential of being successful, dubbed under the name of light stop scenario (LSS) [14]-[30].

The LSS of the MSSM is characterized by a light stop, with a predominantly right-handed component and a mass close to, or smaller than, the top quark mass. All other squarks and sleptons are assumed to be heavier than a few TeV (for example, and for simplicity, acquiring a common mass $\widetilde{m}$) to fulfill the present bounds on the Higgs mass [31]. Large values of $\widetilde{m}$ protect the model against large flavor changing neutral current effects, or unacceptably large CP violation effects and electric dipole moments, but have the drawback of reintroducing a hierarchy problem [1]. On the other hand, the Higgsinos and gauginos are required to be light in order to trigger the required CP-violating currents needed for baryogenesis as well as providing valuable candidate for Dark Matter. Light gauginos and Higgsinos can be technically natural as a consequence of some partly conserved R-symmetry [33].

Large values of $\widetilde{m}$ lead to the subsequent appearance of large logarithms in the one-loop approximation of the Higgs mass used in our previous EWBG calculation [34]. This demands a new treatment of the Effective Theory (ET) of the LSS below $\widetilde{m}$, involving resummation of large logarithms using renormalization group equation techniques, which allows the computation of the Higgs mass in a reliable way [35]. Furthermore, in reference [35] we study the condition of gauge coupling unification in the LSS and find that it predicts values of $\widetilde{m}$ consistent with those required to fulfill the present LEP bounds on the lightest CP-even Higgs mass.

[1] Somewhat reminiscent of the Split Supersymmetry scenario proposed in Refs. [32] although in our case $\widetilde{m}$ may be only moderately large.

In this paper we re-analyze the EWBG capabilities of the LSS in the context of the effective theory presented in Ref. [35]. The article is organized as follows. In section 2 we review the properties of the LSS in some detail and briefly summarize the main results of Ref. [35] relevant for the present study. In particular we describe the features of the low energy theory in which the heavy supersymmetric partners of the quarks and leptons (except for the right-handed stop), as well as the heavy Higgs doublet have been integrated out. In section 3 we discuss the possible cosmological scenarios associated with the phase transition to electroweak and color symmetry breaking vacua. Section 4 contains the numerical results of the parameter space consistent with a sufficiently strong electroweak phase transition. There we present our results as windows in the $(m_H, m_{\tilde{t}})$-plane. We show that the requirement of a strong first-order phase transition provides absolute upper bounds on the Higgs and stop masses, $m_H \lesssim 127$ GeV and $m_{\tilde{t}} \lesssim 120$ GeV, and find that all solutions in these windows correspond to cases where the electroweak vacuum is metastable. The technical details of the effective potentials, in the presence of Higgs and stop background fields, which serve as the basis for the numerical results of section 4, are presented in appendices A and B. In section 5 we study the decay rate of the previously computed metastable electroweak vacua and we show that in all cases their life-time is larger than the life-time of the Universe at all temperatures. We reserve section 6 for our conclusions and outlook.

2 The light stop scenario

The mechanism of electroweak baryogenesis relies on the possible generation of BAU at the electroweak phase transition. To ensure the preservation of the generated baryon asymmetry, the baryon number violating processes must be out of equilibrium at the nucleation temperature T_n. To achieve this, the rate of baryon number violating processes, which depends on the ratio of the sphaleron energy to the critical temperature, must be smaller than the expansion rate of the Universe. Quantitatively, this leads to the condition $\phi(T_n)/T_n \geq 1$, namely a sufficiently strong first-order phase transition [2]. The strength of the phase transition may be analyzed by means of the finite temperature effective potential. It can be shown that strictly speaking the value of $\phi(T_n)/T_n$ is, to a first approximation, directly proportional to the sum of the cube of the couplings of the light bosonic particles of the model to the Higgs boson, and inversely proportional to the quartic Higgs coupling, which is in turn proportional to the square of the Higgs mass. In the SM the only bosonic particles which couple in a relevant way to the Higgs field are the weak gauge bosons, with couplings which are governed by the corresponding weak gauge couplings. The phase transition strength can therefore be evaluated leading to an upper bound on the mass of the Higgs boson about 40 GeV, far below the present LEP lower bounds [3].

[2] We use the convention $\phi(T=0) = v = 246.22$GeV.

[3] The former is a perturbative result. Non-perturbatively, and for allowed Higgs masses, the phase transition has been proved to be a continuous crossover [9].

In the MSSM there are additional bosons with relevant couplings to the Higgs, namely the superpartners of the top quark. Every stop has six degrees of freedom and therefore the stops could contribute relevantly to the phase transition strength leading, for sufficiently light stops, to a strongly first-order phase transition for masses of the Higgs allowed by the present LEP bound, $m_h > 114.7$ GeV [31]. In practice only the (mainly) right-handed stop may be light. The heaviest (mainly) left-handed stop has to acquire a mass above a few TeV to achieve agreement with electroweak precision tests and to ensure a sufficiently heavy Higgs boson [35] compatible with the LEP bounds. On the other hand this favourable improvement on the phase transition would be substantially reduced by gluinos in the plasma due to their potentially large contribution to the effective stop mass at finite temperature, so that gluinos are usually considered heavy enough to be decoupled from the thermal bath. In practice, this implies that the gluino mass should be larger than about 500 GeV.

Another problem for the generation of the BAU within the SM is that the CP-violating sources are highly suppressed. Therefore new sources of CP-violation must be present. In the LSS the CP-violating currents associated with scalar fields are strongly suppressed and therefore the relevant sources may only be generated by the chargino and neutralino currents. The charginos and neutralinos should therefore remain light in this scenario and there should exist non-negligible phases between the Higgsino and gaugino mass parameters μ and M_i, respectively. These phases have important phenomenological consequences inducing potentially large electric dipole moments (EDM) of the electron and the neutron at the one-loop level. The one-loop contributions to the EDM's may be efficiently suppressed if the first and second generation scalar particles are heavy enough, with masses larger than about 10 TeV. Even in the absence of one-loop contributions, two-loop contributions involving the charginos and the Higgs field would remain sizeable [36]. They become, however, smaller for values of the CP-odd Higgs mass larger than about 1 TeV. Still, even for very large values of the CP-odd Higgs mass, there is a contribution induced by the SM-like Higgs boson which, for phases of order one, is only an order of magnitude below the present experimental bounds on the electron electric dipole moment. In the following, we shall identify the CP-odd Higgs mass with $\tilde{m}$.

Summarizing, the generic spectrum of the LSS is constituted by light charginos and neutralinos, a light stop, heavy first and second generation squarks and sleptons and, finally, gluinos much lighter than the heavy scalars but heavy enough to decouple from the thermal bath. In order to lead to agreement with precision data the light stop must be predominantly right-handed, and the left-handed stop should therefore be heavy in order to ensure a large enough Higgs mass. Moreover, even if the LSS has no specific requirement about the Higgs sector, as mentioned above a large splitting between the two Higgs bosons alleviate the MSSM phenomenological problems related to flavor or CP-violating effects, because it mimics at low energy (LE) the Standard Model Higgs sector.

The LSS spectrum contains then light, weak scale particles, as well as heavy massive particles, with masses much higher than the EW scale. On the other hand, EWBG is a

mechanism that works at the EW scale, where heavy particles are decoupled. For that reason it seems appropriate to make the EWBG analysis in the context of the effective theory of the LSS that was studied in Ref. [35] and that we hereby review briefly.

In mass–independent subtraction schemes particle decoupling is usually performed by means of a step-function approximation along with a run-and-match procedure between the underlying theory and the effective one below every decoupling scale. In particular we will work in the $\overline{MS}$-scheme and assume, for simplicity, a common scale $\widetilde{m}$ for all heavy particles. Following this criterion at renormalization scales τ lower than $\widetilde{m}$, at which supersymmetry is broken, the effective Lagrangian turns out to be [35]

$$\begin{aligned}
\mathcal{L}_{eff} &= m^2 H^\dagger H - \frac{\lambda}{2}\left(H^\dagger H\right)^2 - h_t\left[\bar{q}_L \epsilon H^* t_R\right] + Y_t\left[\overline{\tilde{H}}_u \epsilon q_L \tilde{t}_R^*\right] \\
&\quad -\frac{M_3}{2}\Theta_{\tilde{g}}\,\tilde{g}^a\tilde{g}^a - \frac{M_2}{2}\tilde{W}^A\tilde{W}^A - \frac{M_1}{2}\tilde{B}\tilde{B} - \mu\tilde{H}_u^T\epsilon\tilde{H}_d - M_U^2\ \left|\tilde{t}_R\right|^2 \\
&\quad -\sqrt{2}\Theta_{\tilde{g}} G\ \tilde{t}_R\tilde{g}^a\overline{T}^a\overline{t}_R + \sqrt{2}J\ \tilde{t}_R\tilde{B}\overline{t}_R - \frac{1}{6}K\left|\tilde{t}_R\right|^2\left|\tilde{t}_R\right|^2 - Q\ \left|\tilde{t}_R\right|^2|H|^2\ + h.c. \\
&\quad +\frac{H^\dagger}{\sqrt{2}}\left(g_u\sigma^a\tilde{W}^a + g'_u\tilde{B}\right)\tilde{H}_u + \frac{H^T\epsilon}{\sqrt{2}}\left(-g_d\sigma^a\tilde{W}^a + g'_d\tilde{B}\right)\tilde{H}_d + \text{h.c.}\ , \qquad (2.1)
\end{aligned}$$

where m^2, M_U^2 are the Higgs and stop mass parameters, M_i, with $i = 1, 2, 3$ are the masses of the gluinos associated with the hypercharge, weak and strong interactions and μ is the Higgsino mass parameter. The gluino decoupling is taken into account by the symbol $\Theta_{\tilde{g}}$ which is equal to 1 (0) for $\tau \geq M_3$ ($\tau < M_3$). The effective couplings h_t, Y_t, G, J, K, Q, g_u and g_d in Eq. (2.1) are obtained from the RG evolution of their values at the scale $\tilde{m}$ after applying the appropriate one–loop matching conditions [35]

$$\begin{aligned}
Q(\tilde{m}) - \Delta Q &= \left(\lambda_t^2(\tilde{m})\sin^2\beta + \frac{1}{3}\,g'^2(\tilde{m})\cos 2\beta\right)\left(1 - \frac{1}{2}\Delta Z_Q\right)\ , \qquad (2.2)\\
\lambda(\tilde{m}) - \Delta\lambda &= \frac{g^2(\tilde{m}) + g'^2(\tilde{m})}{4}\cos^2 2\beta\left(1 - \frac{1}{2}\Delta Z_\lambda\right)\ , \qquad (2.3)\\
K(\tilde{m}) - \Delta K &= \left(g_3^2(\widetilde{m}) + \frac{4}{3}\,g'^2(\widetilde{m})\right)\left(1 - \frac{1}{2}\Delta Z_K\right), \qquad (2.4)\\
G(\tilde{m}) - \Delta G &= g_3(\tilde{m})\left(1 - \frac{1}{2}\Delta Z_G\right)\ , \qquad (2.5)\\
h_t(\tilde{m}) - \Delta h_t &= \lambda_t(\tilde{m})\sin\beta\left(1 - \frac{1}{2}\Delta Z_{h_t}\right)\ , \qquad (2.6)\\
Y_t(\tilde{m}) - \Delta Y_t &= \lambda_t(\tilde{m})\left(1 - \frac{1}{2}\Delta Z_{Y_t}\right)\ , \qquad (2.7)\\
g_u(\widetilde{m}) = g(\widetilde{m})\sin\beta\ , &\qquad g_d(\widetilde{m}) = g(\widetilde{m})\cos\beta\ , \qquad (2.8)\\
g'_u(\widetilde{m}) = g'(\widetilde{m})\sin\beta\ , &\qquad g'_d(\widetilde{m}) = g'(\widetilde{m})\cos\beta\ , \qquad (2.9)\\
J(\tilde{m}) = \frac{2}{3}g'(\tilde{m})\ . & \qquad (2.10)
\end{aligned}$$

The thresholds ΔQ, $\Delta\lambda$, ΔK, ΔG, Δh_t, ΔY_t and ΔZ_i are computed at one-loop considering only the numerically dominant contributions proportional to the strong gauge coupling

g_3 and the supersymmetric top Yukawa coupling λ_t. In general they are functions of the masses $m^2, M_U^2, M_3, \mu, \widetilde{m}$, the supersymmetric trilinear coupling A_t and the ratio of the two Higgs vacuum expectation values $\tan\beta$ [35]. For instance the most relevant threshold, which already appears at tree–level, is

$$\Delta Q = -\lambda_t^2 \sin^2\beta \frac{\left|\tilde{A}_t\right|^2}{\widetilde{m}^2} \ , \tag{2.11}$$

where $\tilde{A}_t = A_t - \mu\cot\beta$. The relations (2.2)-(2.10) only hold at the decoupling scale $\widetilde{m}$. Below the decoupling scale we need to run the effective couplings following their Renormalization Group Equations (RGE) in the ET [35] down to the EW scale after having crossed the gluino mass scale M_3 at which the gluino, which is the lightest particle to decouple, is integrated out [4]. Since the RGE–evolution resums the (possibly large) leading logarithms our procedure renders reliable the evaluation of the effective couplings and hence the EWBG analysis also for very large values of $\widetilde{m}$.

3 Cosmological scenarios

Due to the large corrections to the effective stop mass at finite temperature, a strong enough phase transition may only be obtained for negative values of the stop mass parameter, $M_U^2 < 0$ [14]. Thus, at zero temperature there are two minima of the effective potential in the (ϕ, U) plane where $\phi = \langle H\rangle$ and $U = \langle\tilde{t}_R\rangle$,be taken into account located at $(\phi_0, 0)$ and $(0, U_0)$ and where the value of the potential is given by $\langle V_H\rangle$ and $\langle V_U\rangle$, respectively. At finite temperature these minima should evolve from the corresponding VEVs $\phi(T)$ and $U(T)$ and their cosmological evolution will strongly depend on the corresponding nucleation temperatures, T_H^n and T_U^n, determined by the tunneling rate from the symmetry preserving vacuum to the electroweak breaking or color breaking vacuum, respectively [5].

There are four possible cosmological scenarios:

Instability region: When $T_U^n > T_H^n$ and $\langle V_H\rangle > \langle V_U\rangle$ the transition from the unbroken phase to the color breaking one happens first and, since the color breaking minimum is deeper than the electroweak minimum, the system will stay in the color breaking minimum forever. This region, that we call "instability region", is of course unrealistic.

[4] The gluino gives rise to new thresholds affecting the RGE and generating discontinuities in the runnings of the low energy couplings and masses. We take its decoupling into account following the expressions obtained in [35].

[5] In order to simplify the different scenarios presented in this section we will identify here the temperature at which the phase transition ends with the nucleation temperature T^n. Our results are not affected by this approximation since a more careful evolution of the phase transitions will be taken into account in the next sections.

Two–step phase transition region: When $T_U^n > T_H^n$ and $\langle V_H \rangle < \langle V_U \rangle$ the transition to the color breaking minimum also happens first but, since the electroweak vacuum is deeper than the color breaking one, the system becomes metastable at a given temperature. If, at a later stage, there were a tunneling transition from the color breaking to the electroweak minimum, the system would supercool and the electroweak phase transition would be much stronger than naively expected. This process was called "two-step phase transition" in Ref. [26]. In Ref. [37] it was proven that the last phase transition never happens, which renders this region unrealistic as well.

Stability region: When $T_U^n < T_H^n$ and $\langle V_H \rangle < \langle V_U \rangle$ the electroweak phase transition happens first and since the electroweak minimum is the true vacuum of the theory this process gives rise to the usual electroweak phase transition. This region is called "stability region" and will be explored in this paper. As we will show, due to the present bounds on the Higgs mass, the electroweak phase transition is too weak in this region for the mechanism of electroweak baryogenesis to take place.

Metastability region: When $T_U^n < T_H^n$ and $\langle V_H \rangle > \langle V_U \rangle$ the electroweak phase transition happens first but the color breaking minimum is deeper than the electroweak minimum, which makes the system to be in a metastable phase. We will call this region "metastability region", which will be the main object of the analysis in the rest of the paper. This scenario will be proven to be viable if the decay rate of the electroweak to the color breaking minimum is slower than the expansion rate of the Universe at the corresponding temperature.

The analysis of the different cosmological scenarios should be done with the help of the effective potential at finite temperature $V(\phi, U; T)$ within the effective theory described in section 2. We have therefore followed the computation of the zero temperature effective potential improved by the one-loop renormalization group equations presented in Ref. [35] and considered the thermal contribution to two-loop order for the ϕ and U fields given in appendix A and B, respectively. We refer the reader to these appendices for the analytical details and we report the numerical results in the next section.

4 Numerical results

In this section we will perform the numerical analysis of the phase transition by using the full effective potential $V(\phi, U; T)$ in the effective theory of section 2 evaluated at a value of the renormalization scale equal to the top-quark pole mass. We will search for fundamental parameter combinations satisfying the following conditions:

1. For baryogenesis requirements the relation $\phi(T_H^n)/T_H^n \geq 1$ must be satisfied. In practice, we shall require the condition $\phi(T_H^c)/T_H^c \geq 0.9$, where the critical temperature T_H^c is the temperature at which the origin and the electroweak minimum

at $\phi(T_H^c)$ are degenerate. This is a conservative requirement since non-perturbative results provide in general a stronger first-order phase transition than perturbative ones [16], and moreover the actual tunneling temperature T_H^n is smaller than T_H^c and the minimum $\phi(T)$ increases fast in the small interval $[T_H^c, T_H^n]$. We will show in section 5 with an specific example that $\phi(T_H^c)/T_H^c \geq 0.9$ induces $\phi(T_H^n)/T_H^n > 1$ within a good approximation.

2. We must impose $T_U^n < T_H^f$, where T_H^f is the temperature at which the electroweak phase transition ends. We thus guarantee that all the bubbles generated during the phase transition are in electroweak symmetry breaking vacua and respect either the stability or metastability conditions. As will be discussed in section 5, the condition $T_U^n < T_H^n$ is fulfilled whenever the much simpler condition $T_H^c \gtrsim T_U^c + 1.6$ GeV is satisfied. Moreover, we find that there are no stability region points consistent with the present bounds on the Higgs mass. Moreover, the metastable vacua satisfying the condition $T_U^n < T_H^f$ do not decay in the lifetime of the Universe, and therefore, provide a good realization of the mechanism of electroweak baryogenesis in the MSSM.

3. The model must be safe from the EDM constraints and generate enough BAU. This is an important requirement since it is known that the generation of BAU requires CP-violating phases of order one. One-loop EDM contributions tend to be suppressed since we have to consider very large values of $\widetilde{m}$, larger than about 10 TeV, to overcome the Higgs mass experimental bound and satisfy the first condition. Also the heavy Higgs sector mass is identified with $\widetilde{m}$, suppressing the two loop contributions to EDM's [36]. However, as previously stressed, there are effects associated to the light SM-like Higgs boson which give contributions which are only one order of magnitude below the present experimental bounds. At a practical level, for smaller values of $\widetilde{m}$ the contributions to the EDM's are enhanced at large values of $\tan\beta$, and strongly depend on $\widetilde{m}$ and on the particular choice of the low energy spectrum.

4. The successful generation of the BAU demands moderate or small values of $\tan\beta$. In practice, there are uncertainties of order one in the theoretical computation of the BAU. At the moment however, large variations on the final results appear from the different approaches [28]–[30] which have been considered in the literature. The different approaches contain advantages and/or disadvantages in the treatment of the CPV currents and sources, the treatment of the diffusion and damping processes and the possible importance of flavor oscillations. These issues are under further study and we expect more conclusive results and comparisons between the different approaches in future publications. The leading contributions to BAU decrease as $1/\tan\beta$ for large values of $\tan\beta$ [28]. Therefore, in order to get an approximate upper bound on the parameter $\tan\beta$ from BAU, in Fig. 1 we plot the ratio of the computed baryon to entropy density ratio η to the one obtained from Big Bang

Nucleosythesis η_{BBN}. We use the formalism of Ref. [28], fixing $\phi(T_H^n)/T_H^n \simeq 1$, $M_1 = M_2 = 200$ GeV,and supposing bubble walls with width $L_w \simeq 20/T$, velocity $v_w \simeq 0.1$ and using the definition $\mu = |\mu| e^{i\phi_\mu}$. The results are only slightly dependent on the stop mass parameters, mainly through the value of $\phi(T_H^n)/T_H^n$. As can be seen Fig. 1, a successful generation of the baryon asymmetry may be obtained provided $\tan\beta \lesssim 15$ or, very conservatively, $\tan\beta \lesssim 5$ (see also Ref. [38]). Furthermore, for values of $\widetilde{m}$ larger than about 10 TeV, the generation of the baryon asymmetry may be obtained without violating the EDM bounds.

The first two conditions stated above mainly depend on the the Higgs quartic coupling λ, the stop quartic coupling K and the stop-Higgs quartic coupling Q, and the Higgs and stop mass parameters. This can be intuitively understood since the barrier developing at finite temperature strongly depends on Q, so that Q is the key parameter for the first

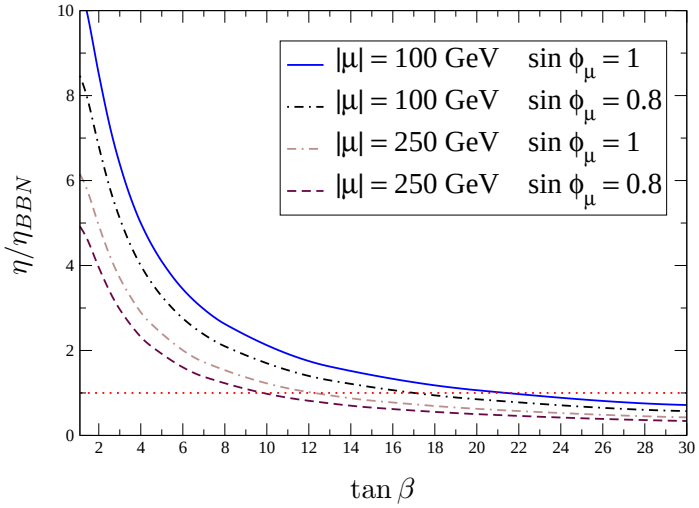

Figure 1: η/η_{BBN} as function of $\tan\beta$ for several values of μ and imposing $\phi(T_H^n)/T_H^n \simeq 1$, $M_1 = M_2 = 200$ GeV, $L_w \simeq 1.7$ and $v_w \simeq 0.1$.

constraint. The remaining parameters determine the depth of the Higgs and stop tree–level potentials and thus they are strictly related to the second condition. In order to compute the values of these parameters, one must fix the parameters $\widetilde{m}$, $\tilde{A}_t$, and $\tan\beta$, as well as require the condition of proper electroweak symmetry breaking. The other free parameters Y_t, μ, M_3, M_2, M_1 only enter through radiative corrections and for this reason we simplify the presentation of our analysis by summarizing the values of the critical low energy parameters as points on the $(m_h, m_{\tilde{t}_R})$ plane, where

$$m^2_{\tilde{t}_R} = M_U^2 + \frac{Q}{2} v^2 \qquad \text{with} \qquad v = 246.22 \text{ GeV}\,, \tag{4.1}$$

and m_h is identified with the second derivative of the one–loop Higgs effective potential in the ET evaluated at Higgs vacuum expectation value v [35]. Notice that $m^2_{t_R}$ in Eq. (4.1) coincides with the (tree–level) stop squared mass in the low–energy effective theory.

In order to determine the window in which EWBG works we perform a scanning on the fundamental parameters at the threshold scale $\widetilde{m}$. Once we fix $\widetilde{m}$ the scanning is performed on $A_t, \tan\beta$ and M_U^2 since they are the parameters that mostly affect the key effective couplings. For the numerical analysis we also have to fix μ, M_1, M_2, M_3. As we have previously explained we shall demand the gluino to be sufficiently heavy to be decoupled from the plasma at the electroweak phase transition. The other parameters are chosen to be at the weak scale, the phase transition strength being only weakly dependent on their specific values.

We shall present the results of the numerical analysis for $M_3 = 500$ GeV and $\mu = M_2 = M_1 = 100$ GeV. Observe that, since we have not included the weak coupling radiative corrections, the Higgs and stop potentials are independent of M_1 and M_2. We shall consider an uncertainty of about ± 3 GeV on our Higgs mass results, reflecting the lack of weak radiative corrections in the Higgs mass computation, as well as uncertainties

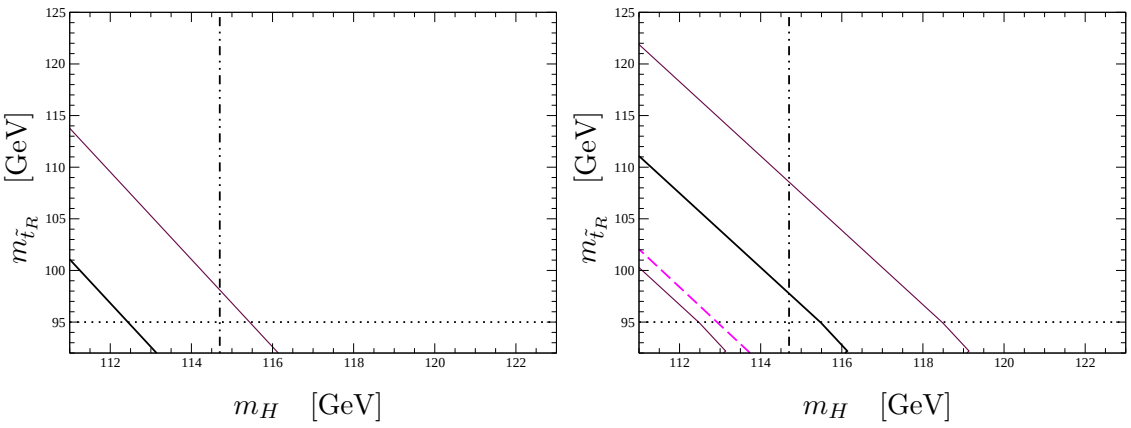

Figure 2: Window where $\phi(T_H^c)/T_H^c \geq 0.9$ and $T_H^c \geq T_U^c + 1.6$ GeV in the m_H-$m_{\tilde{t}}$ plane for $\tilde{m} = 10$ TeV (left panel) and $\tilde{m} = 30$ TeV (right panel). The allowed region is below the solid lines and dashed lines for $\tan\beta \leq 15$ and $\tan\beta \leq 5$, respectively. The thick solid line is obtained by ignoring the Higgs mass uncertainty, while the solid thin lines is obtained by including an uncertainty of 3 GeV in the Higgs mass computation. The Higgs (stop) mass experimental lower bound is marked by a dotted–dashed (dotted) line.

from possible higher-order effects. Under these conditions the allowed windows for the realization of EWBG in the MSSM are shown in Fig. 2, for decoupling scales $\widetilde{m} = 10$ and $\widetilde{m} = 30$ TeV (left and right panels, respectively). The right boundary on each window is provided by the condition $\tan\beta \leq 15$ by black solid thick line ($\tan\beta \leq 5$ by magenta dashed line, only visible in the figure on the right). For the $\tan\beta \leq 15$ case, we draw three

solid lines, corresponding to the bounds on the Higgs mass obtained by ignoring (black solid thick line), as well as considering (maroon solid thin lines) the $\pm$ 3 GeV uncertainty on the Higgs mass discussed above. The allowed area where the condition $\phi(T_H^c)/T_H^c \geq 0.9$ holds is below (to the left of) these boundaries. The Higgs and stop mass experimental lower bounds ($m_h > 114.7\,\text{GeV}$ and $m_{\tilde{t}_R} > 95\,\text{GeV}$ [31]), are marked with dotted and dot-dashed lines, respectively. These results suggest that a heavy squark spectrum of about 10 TeV may be consistent with electroweak baryogenesis only for Higgs boson and stop masses at the edge of the current experimental bounds on these quantities. The situation improves for 30 TeV, for which an upper bound on the Higgs mass of about 118 GeV and on the stop mass of about 110 GeV is obtained.

Fig. 3 shows similar results for extremal values of the decoupling scale $\widetilde{m} = 500$ and $\widetilde{m} = 8000$ TeV, which are still compatible with the condition of gauge coupling unification [35]. The upper almost horizontal border corresponds to points with $A_t = 0$ while going down along the right border the values of A_t are increasing. The lower boundary corresponds to the condition $T_H^c \geq T_U^c + 1.6$ GeV as trespassing this boundary we would fall in the instability or two–step phase transition region. The allowed area where the condition $\phi(T_H^c)/T_H^c \geq 0.9$ holds is inside (to the left of) these solid line boundaries and to the right and above the lines denoting the stop and Higgs mass experimental bounds, respectively. The stop and Higgs boson masses can be extended to larger values for these larger values of $\widetilde{m}$, with an upper bound of about 115 and 124 GeV respectively.

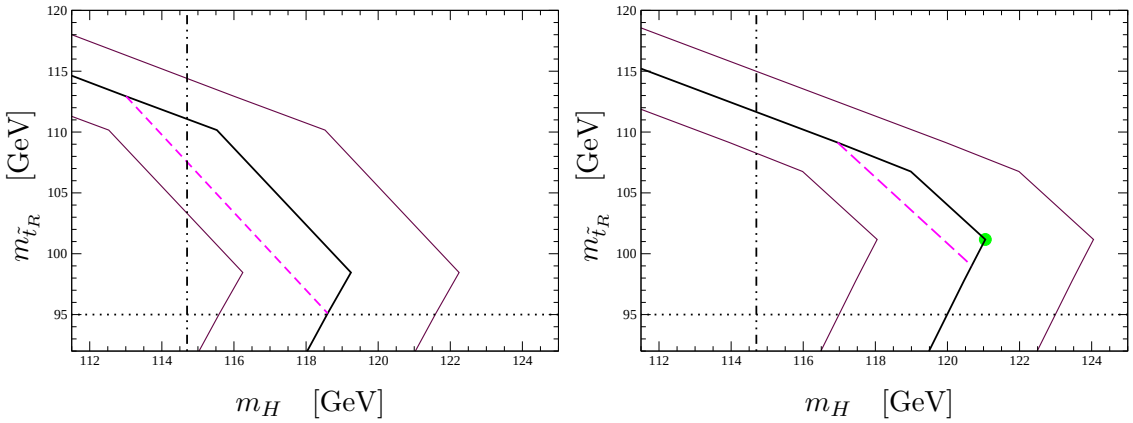

Figure 3: Window where $\phi(T_H^c)/T_H^c \geq 0.9$ and $T_H^c \geq T_U^c + 1.6$ GeV in the m_H-$m_{\tilde{t}}$ plane for $\tilde{m} = 500$ TeV (left panel) and $\tilde{m} = 8000$ TeV (right panel). The allowed region is below the solid lines and dashed lines for $\tan\beta \leq 15$ and $\tan\beta \leq 5$, respectively. The thick solid line is obtained by ignoring the Higgs mass uncertainty, while the solid thin lines is obtained by including an uncertainty of 3 GeV in the Higgs mass computation. The Higgs (stop) mass lower bound is marked by a dotted–dashed (dotted) straight line. In green (right panel) the point that will be numerically analyzed in the tunneling analysis.

Let us now intuitively understand why the window opens for larger values of $\widetilde{m}$. We first consider, at e.g. $\widetilde{m} = 500$ TeV, a point $(m_h, m_{\tilde{t}_R})$ just a bit beyond the right central border of the window. Clearly this point satisfies the first two constraints except that it exceeds a bit the bound $\tan\beta \leq 15$. Let us now increase $\widetilde{m}$ (e.g. to $\widetilde{m} = 8000$ TeV) without changing the other fundamental parameters. As it has been observed in Ref. [35], the value of K increases for larger values of $\widetilde{m}$ implying that the stop tree–level potential becomes less deep and consequently T_U^c decreases. This allows us to consider a larger value of $|M_U^2|$ without loosing the agreement with the second of the requirements $T_H^f > T_U^n$ ($T_H^c > T_U^c + 1.6$ GeV). Observe that the quartic coupling of the Higgs (and therefore the Higgs mass) also increases for larger values of $\widetilde{m}$, but its change is slower than that of K and therefore increasing $\widetilde{m}$ affects much less the critical temperature T_H^c than T_U^c. We have verified that we can then decrease A_t and $\tan\beta$ to recover the previous value of $(m_h, m_{\tilde{t}_R})$ [see formulas (2.11) and (4.1)] by keeping the condition $T_H^f > T_U^n$. Moreover it turns out that by this procedure the cubic term of the potential is larger, so that the phase transition is strengthened and the condition $\phi(T_H^c)/T_H^c \geq 0.9$ can be fulfilled.

The expansion of the windows is shown in Fig. 4 where the maximum value of the Higgs mass (solid and dotted-dashed–dashed lines) [corresponding to the Higgs mass obtained after imposing the upper bound $\tan\beta = 15$ and the maximum available value of $|M_U^2|$ respecting the condition $T_H^c = T_U^c + 1.6$ GeV] and the corresponding value of the light stop mass (dashed line) are plotted as functions of $\widetilde{m}$. The solid lines correspond to the m_h bound obtained by ignoring the 3 GeV theoretical uncertainty, while the dotted-dashed-dashed lines correspond the m_h bounds obtained by considering the theoretical uncertainty. The dotted–dotted-dashed and dotted lines correspond to the m_h and $m_{\tilde{t}}$ experimental mass bounds. Therefore in Fig. 4 the minimum value of $\tilde{m}$ consistent with EWBG in the MSSM can be extracted and it turns out to be $\widetilde{m} \gtrsim 6.5$ TeV, while the maximum value of the Higgs mass is about 127 GeV.

A thorough analysis of the effective potential reveals that all points filling the windows in Figs. 3 and 2 satisfy the condition $\langle V_H \rangle > \langle V_U \rangle$. Therefore they correspond to metastable electroweak vacua. For the above region to be considered as realistic it is necessary to prove that the decay from the electroweak minimum to the (true) color breaking minimum does not happen. This requires to compute the probability of tunneling from the electroweak vacuum to the (deeper) color breaking one. For a point to be considered realistic this tunneling rate should be smaller than the expansion rate of the Universe at all temperatures $T \leq T_H^n$. Due to the similarity between this case and the (inverse) two-step phase transition scenario where a negative result was obtained in Ref. [37], we expect this to be the case. Our numerical results confirm this fact.

5 Analysis of the metastability region

In this section we perform the numerical analysis of the transition to the electroweak breaking phase and the stability of the physical vacuum. The summary of this analysis

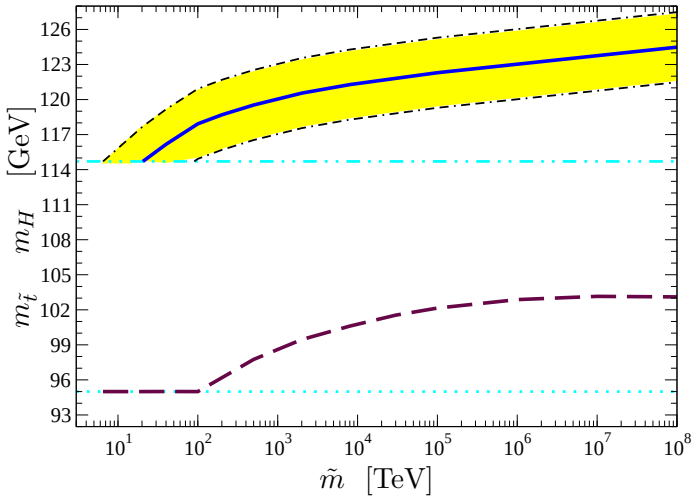

Figure 4: m_H^{max} (upper curves) and the corresponding $m_{\tilde{t}}$ (lower curve) as functions of $\tilde{m}$ for $\phi_c/T_c = 0.9$ and $\tan\beta = 15$ compatible with their corresponding experimental lower mass bounds (dotted–dotted–dashed and dotted lines).

is that as stated above, whenever $T_H^c \gtrsim T_U^c + 1.6$ GeV the electroweak phase transition happens and ends before the color breaking phase transition and the system does not decay to the color breaking minimum in one expansion time of the Universe at any temperature below the nucleation one. We will illustrate it by analyzing a border–line point in the window for $\widetilde{m} = 8000$ TeV which corresponds to the maximum allowed value of the Higgs mass [thick (green) point of Fig. 3].

5.1 Tunneling from the symmetric phase

The tunneling probability per unit time and unit volume from the false (symmetric) to the real (broken) minimum in a thermal bath is given by [39]

$$\frac{\Gamma}{\nu} \sim A(T)\exp\left[-B(T)\right], \quad B(T) \equiv \frac{S_3(T)}{T} \tag{5.1}$$

where the prefactor is $A(T) \simeq T^4$ and S_3 is the three-dimensional effective action. At very high temperature the bounce solution has $O(3)$ symmetry and the euclidean action is simplified to

$$S_3 = 4\pi \int_0^\infty r^2 dr \left[\frac{1}{2}\left(\frac{d\phi}{dr}\right)^2 + V(\phi, T)\right] \tag{5.2}$$

where $r^2 = \vec{x}^2$ and the euclidean equations of motion yield for the bounce solution the equation

$$\frac{d^2\phi}{dr^2} + \frac{2}{r}\frac{d\phi}{dr} = V'(\phi, T) \tag{5.3}$$

with the boundary conditions $\lim_{r\to\infty}\phi(r)=0$ and $d\phi/dr|_{r=0}=0$.

The nucleation temperature T^n is defined as the temperature at which the probability for a bubble to be nucleated inside a horizon volume is of order one and in our case it turns out to happen when $S_3(T^n)/T^n \sim 135$. Below T^n the transition continues until the fraction of the causal horizon in the broken phase is of order one, which can be translated into $S_3(T^f)/T^f \sim 110$ for our case [6, 40] [6].

In Fig. 5 we show the effective potentials (left panel) along the ϕ and U directions at temperatures $T = T_H^c, T_U^c, T_H^n, T_H^f$, with $T_H^c = 128.7$ GeV, $T_U^c = 127.1$ GeV, $T_H^n = 126.0$ GeV and $T_H^f = 125.4$ GeV, for the values of the supersymmetric parameters yielding the maximum value of the Higgs mass in the right panel of Fig. 3. The euclidean actions (right panel) B_H and B_U are computed as function of temperature. At $T = T_H^c = 128.7$ GeV both actions are infinite. At $T = T_U^c$ the action B_U is infinite while the action B_H is still too large. At $T = T_H^n$ the action $B_H \simeq 135$ while $B_U > 135$ which means that the tunneling to the electroweak minimum happens. At $T = T_H^f$ the action $B_H \simeq 110$ while $B_U > 135$ and therefore our universe concludes its electroweak phase transition before the beginning of the colour one.

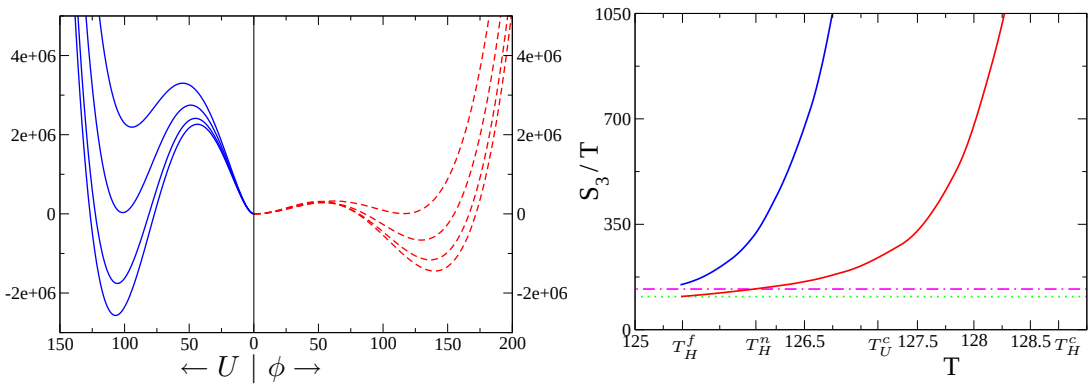

Figure 5: Left panel: effective potential for the Higgs (dashed red lines in the right plot) and stop (solid blue lines in the left plot) fields at temperatures (from top to bottom) $T = T_H^c, T_U^c, T_H^n, T_H^f$(128.7, 127.1, 126.0, 125.4) GeV. Right panel: bounce actions of tunneling from the symmetric phase towards the electroweak (dashed red) and colour (solid blue) breaking minima. The nucleation happens when the action meets the dotted-dashed line and the transition ends when the action crosses the dotted line.

Notice that in this limiting case the rule $T_H^c = T_U^c + 1.6$ GeV is satisfied and, as anticipated, $T_H^f > T_U^n$. In this particular example the difference $T_H^f - T_U^n$ is very small because we are considering a case in the boundary of the instability region, but in all other

[6] We thank Guy Moore for calling our attention into this conceptual point. At a practical level our windows do depend weakly on distinguishing T^n from T^f or on the choice of the numbers used to define them.

points a larger difference $T_H^f - T_U^n$ is found.

The explicitly considered example also shows that the estimate $\phi(T_H^c)/T_H^c = 0.9$ is a conservative one. In particular here we have $T_H^c \approx T_H^n \approx T_H^f$ and $\langle\phi(T_H^n)\rangle \approx \langle\phi(T_H^f)\rangle$ larger than $\langle\phi(T_H^c)\rangle$ by $\mathcal{O}(15\%)$ so that when $\phi(T_H^c)/T_H^c = 0.9$, $\phi(T_H^f)/T_H^f \gtrsim \phi(T_H^n)/T_H^n > 1$ (*i.e.* all the bubbles generated during the phase transition produce a strong first-order transition), which seems to be a general feature in the allowed region.

5.2 Stability of the electroweak minimum

Below the temperature $T = T_H^n$ some regions of the universe are at the electroweak minimum and we must compute the bounce corresponding to the tunneling to the color breaking minimum, B_{HU}, in order to guarantee the stability of the given point. In the following we analyze this for the same point of maximal Higgs mass and $\widetilde{m} = 8000$ TeV studied in the previous section.

In the left panel of Fig. 6 we plot the ϕ and U potentials for temperatures $T = 126,\ 80,\ 0$ GeV and in the right panel we plot the euclidean action $B_{HU}(T)$. We observe that for $T = T_H^n = 126$ GeV the euclidean action is very large. In fact when the temperature drops the action $B_{HU}(T)$ drops to a minimum that nevertheless does not provide a tunneling amplitude that can compete with the expansion rate of the universe. We have checked that this effect is even more accentuated in other non-borderline cases.

Finally notice that our results are based on making a path choice for the bounce B_{HU} that goes through the origin. This path is consistent with the structure of the minima and the behaviour of the potential at tree-level [14] and has been considered to be the proper one to evaluate the transition rate by other similar analyses [26]. For this reason, we believe that our results are reliable.

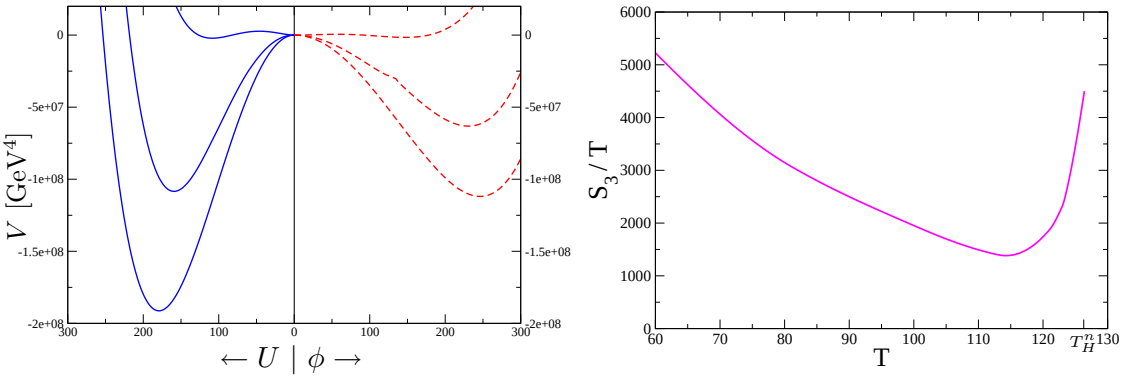

Figure 6: Left panel: Effective potential for the Higgs [dashed red lines in the right plot] and stop [solid blue lines in the left plot] fields at temperatures $T = 126(T_H^n),\ 80,\ 0$ GeV. Right panel: Bounce action B_{HU} from the electroweak to the colour breaking minimum as function of T.

6 Conclusion and outlook

In this article we have analyzed the strength of the EWPT in the LSS, which is the most favourable scenario for EWBG in the MSSM. As it was previously observed in [35] the compatibility between the LSS and the bounds on Higgs and stop masses requires large values of the soft supersymmetry breaking masses. Such large values of the soft masses are also consistent with the condition of gauge coupling unification and are helpful to suppress dangerous flavor changing neutral current and CP-violating effects. Therefore studies on low energy LSS phenomena are reliable only if they are performed in the effective field theory where large leading logarithms are resummed. This effective theory was thoroughly analyzed in Ref. [35] and it has been widely used throughout the present study.

We concentrated on a simple case where all heavy particles (in particular sfermions -except for the right-handed stop- and the non-SM-Higgs sector) have a common mass $\tilde{m}$ while the light ones (fermions and the right-handed stop) have masses at the electroweak scale. In the absence of high energy thresholds, gauge coupling unification predicts values of the scale $\tilde{m}$ which are (depending on the precise value of the gluino mass) in the range $\sim 10^{1-3}$ TeV. This range of $\tilde{m}$ values has some dependence on high energy threshold effects and/or possible mass splittings at the scale $\tilde{m}$.

We have proven that there is a region in the $(\tilde{m}, m_H, m_{\tilde{t}})$ space in which the EWPT is strong enough. The values of $\tilde{m}$ are to a large extent in the same range of values as those predicted by gauge coupling unification. In particular by imposing the LEP bound on the Higgs mass one obtains a lower bound on $\tilde{m} > 6.5$ TeV while for very high values of $\tilde{m}$ one obtains the absolute upper bound on the Higgs mass $m_H \lesssim 127$ GeV. As for the stop mass it has to be light enough in order not to screen the EWPT. Specifically, we have found in all cases an absolute upper bound on the stop mass as $m_{\tilde{t}} \lesssim 120$ GeV.

As we emphasized in section 5, in all points of the allowed BAU windows the electroweak minimum is metastable, while the true minimum would be one where the color and electromagnetic gauge symmetries are spontaneously broken. However we have proven that in all cases the lifetime of tunneling into the color breaking minimum is much larger than the corresponding age of the Universe and so the electroweak minimum is stable.

Searches for a light stop and a light Higgs are under way at the Tevatron collider. The Tevatron can search for a light stop, with mass below 120 GeV, provided the mass difference between the stop and the lightest neutralino (assumed to be the lightest supersymmetric particle) is larger than 30 GeV [41]–[43]. For smaller mass differences, the jets coming from the stop decays are too soft for the Tevatron experiments to trigger on these events, rendering the search ineffective. On the other hand, the existence of a light Higgs, with mass below 127 GeV, may also be probed at the Tevatron collider, provided certain sensitivity improvements can be achieved [43].

A light neutralino within the LSS provides a candidate for dark matter. A proper dark matter relic density may be naturally obtained in the stop-neutralino coannihilation region, associated with stop-neutralino mass differences of about 20 GeV [38]. The stop

will mostly decay into a charm jet and the light neutralino, but due to the smallness of the mass difference it will be beyond the Tevatron reach. The LHC will be able to provide a definitive test of the existence of such a light stop: For gluino masses below about 1 TeV, a light stop may be searched for at the LHC in events with equal sign top-quarks [44, 45]. Even if the gluino mass is larger than 1 TeV, a light stop may be searched for in events with high energy jets or photons and missing energy. This latter search mode, when complemented with Tevatron searches, allows to fully explore the region of stop masses consistent with electroweak baryogenesis [46]. Moreover a light SM-like Higgs may be searched for at the LHC in different production channels and decay modes [47]. Therefore the LHC should be able to provide a definitive test of this scenario within the next few years.

Before concluding, some comments are worthwhile. First, we have considered in this paper the case where the MSSM parameter $m_A \simeq \tilde{m}$ (and thus the low energy Higgs sector is the SM one) because it leads to a suppression of 2-loop induced electric dipole moments, it requires the smallest values of $\tilde{m}$ to obtain a given value of the Higgs mass, and also because its effective theory is more tractable. However there is nothing fundamental in considering this case and one could, following parallel lines to those developed in Ref. [35], also consider the effective theory with two Higgs doublets and analyze the corresponding phase transition and BAU, which favors small values of m_A. The analysis of such a case, although interesting, is outside the scope of the present paper. Second, all phenomena at low energies, and in particular the EWPT, do depend on the parameters of the effective theory which, in turn, depend on the corresponding parameters of the supersymmetric high energy theory. We have chosen a particular configuration for the latter, but other heavy spectra, for instance one in which the heavy third generation sparticle masses are splitted from the first and second one, would lead to similar values of the effective couplings relevant for the EWPT and reproduce similar windows.

Finally, all requirements in the LSS (gauge coupling unification, consistency with EDM experiments, BAU, actual bounds on the Higgs mass) lead to values of the supersymmetry breaking parameter ($\tilde{m} \gtrsim 10$ TeV) where the fine-tuning for triggering the electroweak symmetry breaking is sizeable. Although this fact can be considered as a motivation to go beyond the MSSM, still the possibility of producing the BAU within the MSSM remains as a valid challenge. The existence of a light SM-like Higgs boson and a stop, with masses below 127 GeV and 120 GeV will be probed at the Tevatron and the forthcoming LHC experiments and will provide a crucial test of the EWBG scenario in the MSSM.

Acknowledgments

We would like to thank G. D. Moore and T. Konstandin for useful comments. Work supported in part by the European Commission under the European Union through the Marie Curie Research and Training Networks "Quest for Unification" (MRTN-CT-2004-503369) and "UniverseNet" (MRTN-CT-2006-035863). The work of M.Q. was partly supported

by CICYT, Spain, under contract FPA 2005-02211. Work at ANL is supported in part by the US DOE, Div. of HEP, Contract DE-AC02-06CH11357. Fermilab is operated by Fermi Research Alliance, LLC under Contract No. DE-AC02-07CH11359 with the United States Department of Energy.

Appendix

A Effective potential for the Higgs field

In this appendix we determine the Higgs effective potential at finite temperature including the leading two-loop corrections in the low energy effective theory. We focus in the case where heavy enough gluinos are decoupled from the thermal bath. We will work in the Landau gauge and in the $\overline{\rm MS}$-renormalization scheme. We will fix the $\overline{\rm MS}$-scale τ to the pole top-quark mass and consequently all the effective couplings are evaluated at this scale.

Giving a constant background ϕ_c for the real neutral Higgs boson, the fields of the thermal bath have masses $m_i(\phi_c)$

$$\begin{aligned} m_W^2 &= \frac{g^2}{4}\phi_c^2 \,, \qquad m_Z^2 = \frac{g^2+g'^2}{4}\phi_c^2 \,, \\ m_h^2 &= \frac{\lambda}{2}(3\phi_c^2 - v^2) \,, \qquad m_\chi^2 = \frac{\lambda}{2}(\phi_c^2 - v^2) \,, \\ m_{\tilde{t}_R}^2 &= M_U^2 + \frac{Q}{2}\phi_c^2 \,, \qquad m_t^2 = \frac{h_t^2}{2}\phi_c^2 \,, \end{aligned} \tag{A.1}$$

and degrees of freedom

$$\begin{aligned} n_{W_L} &= 2\,, \qquad n_{W_T} = 4\,, \qquad n_{Z_L} = 1\,, \qquad n_{Z_T} = 2\,, \\ n_{\gamma_L} &= 1\,, \qquad n_{\gamma_T} = 2\,, \qquad n_h = 1\,, \qquad n_\chi = 3\,, \\ & \qquad n_t = -12\,, \qquad n_{\tilde{t}_R} = 6\,. \end{aligned}$$

where the subscript $L(T)$ for gauge bosons is meant for their longitudinal (transverse) degrees of freedom. Moreover it is useful to consider their thermal masses $\overline{m}_i(\phi_c)$

$$\begin{aligned} \overline{m}^2_{Z_L,\gamma_L} &= \frac{1}{2}\left[\frac{1}{4}(g^2+g'^2)\phi_c^2 + \Pi_W + \Pi_B \pm \sqrt{\left((g^2-g'^2)\frac{\phi_c^2}{4} + \Pi_W - \Pi_B\right)^2 + \frac{1}{4}g^2g'^2\phi_c^4}\right] \\ & \overline{m}^2_{W_L} = m_W^2 + \Pi_W\,, \qquad \overline{m}_h^2 = m_h^2 + \Pi_h\,, \\ & \overline{m}^2_{\tilde{t}_R} = m^2_{\tilde{t}_R} + \Pi_{\tilde{t}_R}\,, \qquad \overline{m}_\chi^2 = m_\chi^2 + \Pi_\chi\,, \end{aligned} \tag{A.2}$$

where

$$\begin{aligned}
\Pi_W &= \frac{7}{3} g^2\, T^2\,, \\
\Pi_B &= \frac{22}{9} g'^2\, T^2\,, \\
\Pi_h &= \frac{\lambda}{4}\, T^2 + \frac{5}{16} g^2\, T^2 + \frac{5}{48} g'^2\, T^2 + \frac{1}{2} h_t^2\, T^2\,, \\
\Pi_\chi &= \Pi_h\,, \\
\Pi_{\tilde{t}_R} &= \frac{4}{9} g_s^2\, T^2 + \frac{1}{3} g'^2\, T^2 + \frac{1}{6} Y\, T^2 + \frac{1}{6} Q\, T^2\,.
\end{aligned} \tag{A.3}$$

Considering the Higgs effective potential as a perturbative sum

$$V(\phi_c, T) = V_0 + V_1 + V_2 + \cdots\,, \tag{A.4}$$

where V_n indicates the n-th loop potential in the resummed theory at finite temperature, the tree–level contribution [7] is easily obtained by (2.1) and V_1 is given by

$$V_1(\phi_c, T) = \frac{1}{64\pi^2} \sum_i n_i\; m_i^4(\phi_c) \left(\ln \frac{m_i^2(\phi_c)}{\tau^2} - C_i \right) + \sum_i \frac{n_i}{2\pi^2} J^{(i)} T^4\,, \tag{A.5}$$

where $i = W, Z, h, \chi, \tilde{t}_R, t$ and $C_W = C_Z = 5/6$, $C_h = C_\chi = C_{\tilde{t}_R} = C_t = 3/2$ [8]. Since we perform daisy resummation on the $n = 0$ modes of the longitudinal components of the gauge bosons W_L, Z_L, γ_L and of the scalar bosons h, χ, $\tilde{t}_R$ (no resummation on fermions), the thermal contributions $J^{(i)}$ are defined by

$$J^{(i)} = \begin{cases} J_B(m_i^2) - \dfrac{\pi}{6} \left(\overline{m}_i^3 - m_i^3 \right) & i = W_L, Z_L, \gamma_L, h, \chi, \tilde{t}_R \\ \\ J_B(m_i^2) & i = W_T, Z_T, \widetilde{T} \\ \\ J_F(m_i^2) & i = t \end{cases} \tag{A.6}$$

where the thermal integrals $J_{B,F}$ are

$$J_{B,F}(y^2) = \int_0^\infty dx\; x^2 \log \left(1 \mp e^{-\sqrt{x^2 + y^2}} \right)\,. \tag{A.7}$$

We also take into account the logarithmic contributions [9] coming from the two-loop potential proportional to effective couplings related to g_3 and λ_t in their matching condition

[7] The tree level Higgs mass is defined such as the one–loop Higgs potential has a minimum at $v = 246.22$ GeV.

[8] Notice that we are only considering for simplicity the leading contribution of fields beyond the SM. The subleading contribution from Higgsinos and/or weak gauginos would not modify the results in a substantial amount.

[9] It was observed in Ref. [21] that non-logarithmic contributions are negligible in the study of the phase transition.

(2.2)-(2.10). In this approximation the relevant terms are the sunset diagrams, labeled by V_{XYZ}, where X, Y and Z are the propagating fields, and figure eight diagrams, labeled by V_{XY}, with propagating X and Y fields. With this prescription the two-loop potential turns out to be

$$V_2 = V_{\tilde{t}_R\tilde{t}_R g} + V_{\tilde{t}_R\tilde{t}_R h} + V_{g\tilde{t}_R} + V_{\tilde{t}_R h} + V_{\tilde{t}_R\chi} + V_{\tilde{t}_R\tilde{t}_R} \ , \tag{A.8}$$

where g stands for gluons and the different contributions are given by

$$\begin{aligned}
V_{\tilde{t}_R\tilde{t}_R\, g} &= -\frac{g_s^2}{4}(N_c^2-1)\mathcal{D}_{SSV}(\overline{m}_{\tilde{t}_R}, \overline{m}_{\tilde{t}_R}, 0) \\
V_{\tilde{t}_R\tilde{t}_R\, h} &= -\frac{1}{2}Q^2\phi_c^2 T^2 N_c H(\overline{m}_h, \overline{m}_{\tilde{t}_R}, \overline{m}_{\tilde{t}_R}) \\
V_{g\tilde{t}_R} &= -\frac{g_s^2}{4}(N_c^2-1)\mathcal{D}_{SV}(\overline{m}_{\tilde{t}_R}, 0) \\
V_{\tilde{t}_R\, h} &= \frac{1}{2}Q^2 \sin^2\beta\ N_c\ I(\overline{m}_{\tilde{t}_R})\, I(\overline{m}_h) \\
V_{\tilde{t}_R\,\chi} &= \frac{3}{2}Q^2 \sin^2\beta\ N_c\ I(\overline{m}_{\tilde{t}_R})\, I(\overline{m}_\chi) \\
V_{\tilde{t}_R\tilde{t}_R} &= \frac{K}{6}N_c(N_c+1)\ I^2(\overline{m}_{\tilde{t}_R}))
\end{aligned} \tag{A.9}$$

The functions involved in (A.9) are all defined in Ref. [8].

The Higgs potential we have just described is well defined only for temperatures so large that all squared masses are positive for any ϕ_c. When we need to consider lower temperatures, for what concerns V_1 we expand the thermal integrals $J_{B,F}$ [48] and we consider the real part of V_1 [49] while for V_2 we use the approximation

$$V_2 \simeq \frac{(\phi_c/T)^2}{32\pi^2}\left[\frac{51}{16}g_2^2 - 3Q^2 + 8g_3^2 Q \log\left(\kappa_H \frac{T}{|m_{\tilde{t}_R}|}\right)\right] \tag{A.10}$$

where $\kappa_H \simeq 2.3$.

B Effective potential for the stop field

In this appendix we will compute the effective potential at finite temperature in the background field $U \equiv \tilde{t}_R^\alpha u_\alpha$, where u_α is a constant unit vector in color space which breaks $SU(3)_c$ into $SU(2)$. We will proceed as in appendix A and present the result of the two-loop calculation following the same approximations used for the Higgs potential.

The states contributing to the effective potential are the gauge boson B, four gluons C and the gluon C', five real squarks ω (would-be Goldstones) and the real squark ρ, the Higgs H and two massive Dirac fermions f coming from the mixing between the left-handed (third generation) fermion doublet $q_L \equiv q_L^\alpha u_\alpha$ and the Higgsino, with the

corresponding degrees of freedom

$$\begin{aligned} &n_{C_L} = 4\,, \qquad n_{C_T} = 8\,, \qquad n_{C'_L} = 1\,, \qquad n_{C'_T} = 2\,, \\ &n_{B_L} = 1\,, \qquad n_{B_T} = 2\,, \qquad n_H = 4\,, \qquad n_\omega = 5\,, \\ &\qquad\qquad n_\rho = 1\,, \qquad n_f = -8\,. \end{aligned} \tag{B.1}$$

Their masses in the background U are

$$\begin{aligned} m_B^2 = \frac{8}{9} g'^2 U^2\,, \qquad m_C^2 = \frac{1}{2} g_s^2 U^2\,, \qquad m_{C'}^2 = \frac{2}{3} g_s^2 U^2\,, \\ m_\omega^2 = M_U^2 + \frac{1}{3} K U^2\,, \qquad m_\rho^2 = M_U^2 + K U^2\,, \qquad m_H^2 = m_h^2 + Q U^2\,, \\ m_f^2 = \mu^2 + Y^2 U^2\,, \end{aligned} \tag{B.2}$$

while their thermal masses are defined as $\overline{m}_i^2 = m_i^2 + \Pi_i$ where $\Pi_\omega = \Pi_\rho = \Pi_{\tilde{t}_R}$ and $\Pi_H = \Pi_h$.

The one–loop contribution can be written as expressed in (A.5), where now the index i runs over $B, C, C', \omega, \rho, H, f$ and the functions $J^{(i)}$ are defined by

$$J^{(i)} = \begin{cases} J_B(m_i^2) - \dfrac{\pi}{6}\left(\overline{m}_i^3 - m_i^3\right) & i = B_L, \omega, \rho, H \\ \\ J_B(m_i^2) & i = B_T, C_T, C'_T, \mathcal{Q} \\ \\ J_F(m_i^2) & i = f\ . \end{cases} \tag{B.3}$$

For the functions $J^{C,C'}$ we use their high temperature expansion except for the contribution of the zero mode (cubic term) which is screened by the large thermal correction to its mass $\Pi_{C,C'} = \frac{8}{3} g_s^2 T^2$.

Finally the two-loop diagrams which contribute to V_2 are of two kinds: sunset diagrams labeled by V_{XYZ}, where X, Y and Z are propagating fields, and figure eight diagrams labeled by V_{XY}, with propagating X and Y fields. In the following we will denote $\mathcal{C} \equiv (C, C')$ and $\tilde{t}_R \equiv (\omega, \rho)$, η being the ghost fields. Under this prescription V_2 is given by

$$
\begin{aligned}
V_{CCC} &= -g_s^2\frac{N_c}{4}\left[(N_c-2)\mathcal{D}_{VVV}(m_C,m_C,0)+\mathcal{D}_{VVV}(m_C,m_C,m_{C'})\right] \\
V_{\eta\eta C} &= -g_s^2\frac{N_c}{2}\left[2(N_c-1)\mathcal{D}_{\eta\eta V}(0,0,m_C)+\mathcal{D}_{\eta\eta V}(0,0,m_{C'})\right] \\
V_{\tilde{t}_R\tilde{t}_R C} &= -\frac{g_s^2}{4}\left[(N_c-1)\mathcal{D}_{SSV}(\overline{m}_\omega,\overline{m}_\omega,m_C)+(N_c-1)\mathcal{D}_{SSV}(\overline{m}_\omega,\overline{m}_\rho,m_C)\right. \\
&+ \frac{N_c-1}{N_c}\mathcal{D}_{SSV}((\overline{m}_\omega,\overline{m}_\rho,m_{C'})+\frac{1}{N_c}\mathcal{D}_{SSV}\mathcal{D}_{SSV}(\overline{m}_\omega,\overline{m}_\omega,m_{C'}) \\
&+ \left. N_c(N_c-2)(\overline{m}_\omega,\overline{m}_\omega,0)\right] \\
V_{\tilde{t}_R CC} &= -g_s^2\frac{m_C^2}{8}\left[(N_c-1)\mathcal{D}_{SSV}(\overline{m}_\rho,m_C,m_C)+2\frac{(N_c-1)^2}{N_c^2}\mathcal{D}_{SSV}(\overline{m}_\rho,m_{C'},m_{C'})\right. \\
&+ \left.\frac{(N_c-2)^2}{N_c}\mathcal{D}_{SSV}(\overline{m}_\omega,m_C,m_{C'})+N_c(N_c-2)\mathcal{D}_{SSV}(\overline{m}_\omega,m_C,0)\right]
\end{aligned}
\tag{B.4}
$$

$$
\begin{aligned}
V_{GG} &= -g_s^2\frac{N_c}{8}\left[2(N_c-2)\mathcal{D}_{VV}(0,m_C)+2\mathcal{D}_{VV}(m_C,m_{C'})+(N_c-1)\mathcal{D}_{VV}(m_C,m_C)\right] \\
V_{\tilde{t}_R G} &= -\frac{g_s^2}{8}\left\{(N_c-1)\left[3\mathcal{D}_{SV}(\overline{m}_\omega,m_C)+\mathcal{D}_{SV}(\overline{m}_\rho,m_C)\right]\right. \\
&+ \frac{1}{N_c}\left[(N_c+1)\mathcal{D}_{SV}(\overline{m}_\omega,m_{C'})+(N_c-1)\mathcal{D}_{SV}(\overline{m}_\rho,m_{C'})\right] \\
&+ \left. 2N_c(N_c-2)(\overline{m}_\omega,0)\right\} \\
V_{\tilde{t}_R\tilde{t}_R\tilde{t}_R} &= -\frac{K^2}{18}\left[3H(\overline{m}_\rho,\overline{m}_\rho,\overline{m}_\rho)+(2N_c-1)H(\overline{m}_\rho,\overline{m}_\omega,\overline{m}_\omega)\right]\,T^2\,U^2 \\
V_{\tilde{t}_R HH} &= -2Q^2UT^2H(\overline{m}_\omega,\overline{m}_H,\overline{m}_H)\,T^2 \\
V_{\tilde{t}_R\tilde{t}_R} &= \frac{1}{24}K\left[3I^2(\overline{m}_\rho)+(4N_c-2)I(\overline{m}_\rho)I(\overline{m}_\rho)+(4N_c^2-1)I^2(\overline{m}_\omega)\right] \\
V_{\tilde{t}_R H} &= Q\;I(\overline{m}_H)\left[I(\overline{m}_\rho)+(2N_c-1)I(\overline{m}_\omega)\right]
\end{aligned}
$$

where all functions involved in (B.4) are defined in Ref. [8].

At low temperatures the potential we have just constructed has problems as the Higgs effective potential (see appendix A). Also in this case we extract the real part from the one–loop contribution V_1 and we approximate the two–loop part V_2 as follows

$$
V_2 \simeq \frac{(U/T)^2}{16\pi^2}\left[\frac{100}{9}g_2^2-2Q^2\log\left(\kappa_U\frac{T}{U}\right)\right]\,, \tag{B.5}
$$

where empirically $\kappa_U \simeq 1.7$.

References

[1] A.D. Sakharov, JETP Lett.**6**, 24 (1967).

[2] G. 't Hooft, Phys. Rev. Lett. **37**, 8 (1976); Phys. Rev. D **14**, 3432 (1976) [Erratum-ibid. D **18**, 2199 (1978)].

[3] P. Arnold and L. D. McLerran, Phys. Rev. D **36**, 581 (1987); Phys. Rev. D **37**, 1020 (1988); S. Y. Khlebnikov and M. E. Shaposhnikov, Nucl. Phys. B **308**, 885 (1988). F. R. Klinkhamer and N. S. Manton, Phys. Rev. D **30**, 2212 (1984); B. M. Kastening, R. D. Peccei and X. Zhang, Phys. Lett. B **266**, 413 (1991); L. Carson, X. Li, L. D. McLerran and R. T. Wang, Phys. Rev. D **42**, 2127 (1990); M. Dine, P. Huet and R. L. Singleton, Nucl. Phys. B **375**, 625 (1992);

[4] For some reviews, see: A. G. Cohen, D. B. Kaplan and A. E. Nelson, Ann. Rev. Nucl. Part. Sci. **43**, 27 (1993) [arXiv:hep-ph/9302210]; M. Quiros, Helv. Phys. Acta **67**, 451 (1994); V. A. Rubakov and M. E. Shaposhnikov, Usp. Fiz. Nauk **166**, 493 (1996) [Phys. Usp. **39**, 461 (1996)] [arXiv:hep-ph/9603208]; M. S. Carena and C. E. M. Wagner, arXiv:hep-ph/9704347.

[5] M. E. Shaposhnikov, JETP Lett. **44**, 465 (1986) [Pisma Zh. Eksp. Teor. Fiz. **44**, 364 (1986)]; Nucl. Phys. B **287**, 757 (1987) and **B299** (1988) 797.

[6] G. W. Anderson and L. J. Hall, Phys. Rev. D **45**, 2685 (1992).

[7] M. E. Carrington, Phys. Rev. D **45**, 2933 (1992); M. Dine, R. G. Leigh, P. Huet, A. D. Linde and D. A. Linde, Phys. Lett. B **283**, 319 (1992) [arXiv:hep-ph/9203201]; Phys. Rev. D **46**, 550 (1992) [arXiv:hep-ph/9203203]; J. R. Espinosa, M. Quiros and F. Zwirner, Phys. Lett. B **314**, 206 (1993) [arXiv:hep-ph/9212248]; W. Buchmuller, Z. Fodor, T. Helbig and D. Walliser, Annals Phys. **234**, 260 (1994) [arXiv:hep-ph/9303251].

[8] P. Arnold and O. Espinosa, Phys. Rev. D **47**, 3546 (1993) [Erratum-ibid. D **50**, 6662 (1994)] [arXiv:hep-ph/9212235].

[9] K. Kajantie, K. Rummukainen and M. E. Shaposhnikov, Nucl. Phys. B **407**, 356 (1993) [arXiv:hep-ph/9305345]; Z. Fodor, J. Hein, K. Jansen, A. Jaster and I. Montvay, Nucl. Phys. B **439**, 147 (1995) [arXiv:hep-lat/9409017]; K. Kajantie, M. Laine, K. Rummukainen and M. E. Shaposhnikov, Nucl. Phys. B **466**, 189 (1996) [arXiv:hep-lat/9510020]; K. Jansen, Nucl. Phys. Proc. Suppl. **47**, 196 (1996) [arXiv:hep-lat/9509018]. For an alternative approach, see: B. Bergerhoff and C. Wetterich, Nucl. Phys. B **440**, 171 (1995) [arXiv:hep-ph/9409295] and references therein.

[10] G. R. Farrar and M. E. Shaposhnikov, Phys. Rev. Lett. **70**, 2833 (1993) [Erratum-ibid. **71**, 210 (1993)] [arXiv:hep-ph/9305274]; M. B. Gavela, P. Hernandez, J. Orloff and O. Pene, Mod. Phys. Lett. A **9**, 795 (1994) [arXiv:hep-ph/9312215]; M. B. Gavela, P. Hernandez, J. Orloff, O. Pene and C. Quimbay, Nucl. Phys. B **430**, 382 (1994) [arXiv:hep-ph/9406289]; P. Huet and E. Sather, Phys. Rev. D **51**, 379 (1995) [arXiv:hep-ph/9404302].

[11] G. F. Giudice, Phys. Rev. D **45**, 3177 (1992); K. S. Myint, Nucl. Phys. A **547**, 227C (1992).

[12] J. R. Espinosa, M. Quiros and F. Zwirner, Phys. Lett. B **307**, 106 (1993) [arXiv:hep-ph/9303317].

[13] A. Brignole, J. R. Espinosa, M. Quiros and F. Zwirner, Phys. Lett. B **324**, 181 (1994) [arXiv:hep-ph/9312296].

[14] M. S. Carena, M. Quiros and C. E. M. Wagner, Phys. Lett. B **380**, 81 (1996) [arXiv:hep-ph/9603420].

[15] D. Delepine, J. M. Gerard, R. Gonzalez Felipe and J. Weyers, Phys. Lett. B **386**, 183 (1996) [arXiv:hep-ph/9604440].

[16] J. M. Cline and K. Kainulainen, Nucl. Phys. B **482**, 73 (1996) [arXiv:hep-ph/9605235]; Nucl. Phys. B **510**, 88 (1998) [arXiv:hep-ph/9705201]; M. Laine and K. Rummukainen, Nucl. Phys. B **535**, 423 (1998) [arXiv:hep-lat/9804019]; Phys. Rev. Lett. **80**, 5259 (1998) [arXiv:hep-ph/9804255].

[17] M. Laine, Nucl. Phys. B **481**, 43 (1996) [Erratum-ibid. B **548**, 637 (1999)] [arXiv:hep-ph/9605283]; M. Losada, Phys. Rev. D **56**, 2893 (1997) [arXiv:hep-ph/9605266]; preprint arXiv:hep-ph/9612337; G. R. Farrar and M. Losada, Phys. Lett. B **406**, 60 (1997) [arXiv:hep-ph/9612346].

[18] J. R. Espinosa, Nucl. Phys. B **475**, 273 (1996) [arXiv:hep-ph/9604320].

[19] B. de Carlos and J. R. Espinosa, Nucl. Phys. B **503**, 24 (1997) [arXiv:hep-ph/9703212].

[20] M. S. Carena, M. Quiros, A. Riotto, I. Vilja and C. E. M. Wagner, Nucl. Phys. B **503**, 387 (1997) [arXiv:hep-ph/9702409].

[21] M. S. Carena, M. Quiros and C. E. M. Wagner, Nucl. Phys. B **524**, 3 (1998) [arXiv:hep-ph/9710401].

[22] J. M. Cline, M. Joyce and K. Kainulainen, Phys. Lett. B **417**, 79 (1998) [Erratum-ibid. B **448**, 321 (1999)] [arXiv:hep-ph/9708393].

[23] T. Multamaki and I. Vilja, Phys. Lett. B **411**, 301 (1997) [arXiv:hep-ph/9705469].

[24] A. Riotto, Int. J. Mod. Phys. D **7**, 815 (1998) [arXiv:hep-ph/9709286].

[25] M. P. Worah, Phys. Rev. D **56**, 2010 (1997) [arXiv:hep-ph/9702423].

[26] D. Bodeker, P. John, M. Laine and M. G. Schmidt, Nucl. Phys. B **497**, 387 (1997) [arXiv:hep-ph/9612364].

[27] J. M. Cline and K. Kainulainen, Phys. Rev. Lett. **85**, 5519 (2000) [arXiv:hep-ph/0002272]; J. M. Cline, M. Joyce and K. Kainulainen, JHEP **0007**, 018 (2000) [arXiv:hep-ph/0006119].

[28] M. S. Carena, J. M. Moreno, M. Quiros, M. Seco and C. E. M. Wagner, Nucl. Phys. B **599**, 158 (2001) [arXiv:hep-ph/0011055]; M. S. Carena, M. Quiros, M. Seco and C. E. M. Wagner, Nucl. Phys. B **650**, 24 (2003) [arXiv:hep-ph/0208043].

[29] T. Konstandin, T. Prokopec, M. G. Schmidt and M. Seco, Nucl. Phys. B **738**, 1 (2006) [arXiv:hep-ph/0505103].

[30] V. Cirigliano, S. Profumo and M. J. Ramsey-Musolf, JHEP **0607**, 002 (2006) [arXiv:hep-ph/0603246].

[31] W. M. Yao *et al.* [Particle Data Group], J. Phys. G **33** 1 (2006).

[32] N. Arkani-Hamed, S. Dimopoulos, G. F. Giudice and A. Romanino, Nucl. Phys. B **709** 3 (2005) [arXiv:hep-ph/0409232]; G. F. Giudice and A. Romanino, Nucl. Phys. B **699** 65 (2004) [Erratum-ibid. B **706** 65 (2005)] [arXiv:hep-ph/0406088].

[33] See, for example, I. Antoniadis, AIP Conf. Proc. **805**, 219 (2006) [arXiv:hep-th/0510037]; I. Antoniadis, K. Benakli, A. Delgado, M. Quiros and M. Tuckmantel, Nucl. Phys. B **744**, 156 (2006) [arXiv:hep-th/0601003].

[34] M. S. Carena, J. R. Espinosa, M. Quiros and C. E. M. Wagner, Phys. Lett. B **355** 209 (1995) [arXiv:hep-ph/9504316]; M. S. Carena, M. Quiros and C. E. M. Wagner, Nucl. Phys. B **461** 407 (1996) [arXiv:hep-ph/9508343].

[35] M. Carena, G. Nardini, M. Quiros and C. E. M. Wagner, arXiv:0806.4297 [hep-ph].

[36] A. Pilaftsis, Nucl. Phys. B **644**, 263 (2002) [arXiv:hep-ph/0207277]; D. Chang, W. F. Chang and W. Y. Keung, Phys. Rev. D **71**, 076006 (2005) [arXiv:hep-ph/0503055]; G. F. Giudice and A. Romanino, Phys. Lett. B **634**, 307 (2006) [arXiv:hep-ph/0510197]; Y. Li, S. Profumo and M. Ramsey-Musolf, arXiv:0806.2693 [hep-ph].

[37] J. M. Cline, G. D. Moore and G. Servant, Phys. Rev. D **60** 105035 (1999) [arXiv:hep-ph/9902220].

[38] C. Balázs, M. Carena and C. E. M. Wagner, Phys. Rev. D **70**, 015007 (2004);
C. Balázs, M. Carena, A. Menon, D. E. Morrissey and C. E. M. Wagner, Phys. Rev. D **71**, 075002 (2005).

[39] A. D. Linde, Nucl. Phys. B **216** 421 (1983) [Erratum-ibid. B **223** 544 (1983)].

[40] A. H. Guth and S. H. H. Tye, Phys. Rev. Lett. **44**, 631 (1980) [Erratum-ibid. **44**, 963 (1980)], A. H. Guth and E. J. Weinberg, Phys. Rev. D **23**, 876 (1981), S. J. Huber and T. Konstandin, JCAP **0805**, 017 (2008) [arXiv:0709.2091 [hep-ph]].

[41] V. M. Abazov *et al.* [DØ Collaboration], Phys. Lett. B **665**, 1 (2008).

[42] N. Bhattacharyya, A. Datta and M. Maity, arXiv:0807.0994 [hep-ph].

[43] [CDF and D0 Collaborations], Report to the Particle Physics Project Prioritization Panel: *The Case for Run II* (2005), `http://www-cdf.fnal.gov/physics/projections/`.

[44] S. Kraml and A. R. Raklev, Phys. Rev. D **73**, 075002 (2006);
S. Kraml and A. R. Raklev, AIP Conf. Proc. **903**, 225 (2007) [hep-ph/0609293].

[45] S. P. Martin, arXiv:0807.2820 [hep-ph].

[46] M. Carena, A. Freitas and C. E. M. Wagner, arXiv:0808.2298 [hep-ph].

[47] See, for example, L. R. Flores-Castillo [ATLAS and CMS Collaborations], Nucl. Phys. Proc. Suppl. **177-178**, 229 (2008).

[48] L. Dolan and R. Jackiw, Phys. Rev. D **9**, 3320 (1974).

[49] E. J. Weinberg and A. q. Wu, Phys. Rev. D **36**, 2474 (1987).